Point Pairing Method Based on the Principle of Material Frame Indifference for the Characterization of Unknown Space Objects using Non-Resolved Photometry Data

Anil B. Chaudhary, Tamara E. Payne, Keith Lucas, Shaylah Mutschler, Tim Vincent
Applied Optimization, Inc.
Phan Dao, Jeremy Murray-Krezan
Air Force Research Laboratory /RVBY

ABSTRACT

The *point pairing* method in this paper is based on a set of simple physical truths for three-axis stabilized space objects in the geosynchronous orbit (GEO). It defines a method for the calculation of pairs of observation conditions (i.e. point pairs) that have a special property for three-axis stabilized GEO object characterization. An observation condition is defined to be the geometry of illumination for the solar panel and the body of the satellite and the geometry of its observation by a sensor. The physical truths are due to observation conditions that are equivalent with respect to either the solar panel or body for a pair of points, which can be identified analytically. When the observation conditions are equivalent for the solar panel, the contribution to the GEO object brightness by the solar panel at that pair of points is identical. Then the difference between the pair of brightness values cancels the solar panel contribution unconditionally, and the remainder is only due to the body. Similarly, when the contribution of the body to the observed brightness is the same for the point pair, the difference between the two brightness values cancels the body contribution unconditionally and the remainder is only due to the solar panels. This enables separation of the observed brightness data into contributions by the solar panels and the body, which is fundamental to space-object characterization. This separation of the solar panel or body contributions is feasible in each waveband of observation. Thus point pairing is useful for the analysis of panchromatic as well as multi-spectral data. The desired conditions for point pairing occur routinely, typically within weeks of each other.

1. INTRODUCTION

The principle of material frame indifference (PMFI) is one of the basic principles in the mechanics of materials that is utilized for the characterization of the intrinsic, physical, constitutive behavior of materials. Reference [1] describes this principle as follows: "Physical laws, if they really describe the physical world, should be independent of the position and orientation of the observer. That is, if two scientists using different coordinate systems observe the same physical point, it should be possible to state a physical law governing the event in such a way that if the law is true for one observer, it is also true for the other. For this reason, the equations of physical laws are vector equations or tensor equations, since vectors and tensors transform from one coordinate system to another in such a way that if a vector of a tensor equation holds in one coordinate system, it holds in any other coordinate system not moving relative to the first one, i.e., in any other coordinate system in the same reference frame."

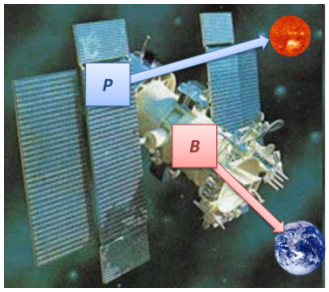

Fig. 1-1: Nadir Facing 3-Axis Stabilized Body and Sunward Articulating Solar Panels

The present paper applies PMFI to analyze the reflection of incident sunlight by a space object and to determine conditions under which the observations taken at two distinct instants of time possess a special property that is

Report Documentation Page

Form Approved
OMB No. 0704-0188

1. REPORT DATE	2. REPORT TYPE	3. DATES COVERED
SEP 2013		**00-00-2013 to 00-00-2013**

4. TITLE AND SUBTITLE	5a. CONTRACT NUMBER
Point Pairing Method Based on the Principle of Material Frame Indifference for the Characterization of Unknown Space Objects using Non-Resolved Photometry Data	5b. GRANT NUMBER
	5c. PROGRAM ELEMENT NUMBER
6. AUTHOR(S)	5d. PROJECT NUMBER
	5e. TASK NUMBER
	5f. WORK UNIT NUMBER
7. PERFORMING ORGANIZATION NAME(S) AND ADDRESS(ES) **Air Force Research Laboratory (AFRL),Space Vehicles Directorate (RVBY),Kirtland AFB,NM,87117**	8. PERFORMING ORGANIZATION REPORT NUMBER
9. SPONSORING/MONITORING AGENCY NAME(S) AND ADDRESS(ES)	10. SPONSOR/MONITOR'S ACRONYM(S)
	11. SPONSOR/MONITOR'S REPORT NUMBER(S)

12. DISTRIBUTION/AVAILABILITY STATEMENT
Approved for public release; distribution unlimited

13. SUPPLEMENTARY NOTES
2013 AMOS (Advanced Maui Optical and Space Surveillance) Technical Conference, 10-13 Sep, Maui, HI.

14. ABSTRACT
The point pairing method in this paper is based on a set of simple physical truths for three-axis stabilized space objects in the geosynchronous orbit (GEO). It defines a method for the calculation of pairs of observation conditions (i.e. point pairs) that have a special property for three-axis stabilized GEO object characterization. An observation condition is defined to be the geometry of illumination for the solar panel and the body of the satellite and the geometry of its observation by a sensor. The physical truths are due to observation conditions that are equivalent with respect to either the solar panel or body for a pair of points, which can be identified analytically. When the observation conditions are equivalent for the solar panel, the contribution to the GEO object brightness by the solar panel at that pair of points is identical. Then the difference between the pair of brightness values cancels the solar panel contribution unconditionally, and the remainder is only due to the body. Similarly, when the contribution of the body to the observed brightness is the same for the point pair, the difference between the two brightness values cancels the body contribution unconditionally and the remainder is only due to the solar panels. This enables separation of the observed brightness data into contributions by the solar panels and the body, which is fundamental to space-object characterization. This separation of the solar panel or body contributions is feasible in each waveband of observation. Thus point pairing is useful for the analysis of panchromatic as well as multispectral data. The desired conditions for point pairing occur routinely, typically within weeks of each other.

15. SUBJECT TERMS

16. SECURITY CLASSIFICATION OF:			17. LIMITATION OF ABSTRACT	18. NUMBER OF PAGES	19a. NAME OF RESPONSIBLE PERSON
a. REPORT **unclassified**	b. ABSTRACT **unclassified**	c. THIS PAGE **unclassified**	**Same as Report (SAR)**	**14**	

Standard Form 298 (Rev. 8-98)
Prescribed by ANSI Std Z39-18

useful in the analysis of non-resolved photometric data. The two materials of interest are those that constitute the solar panel and the body of a 3-axis stabilized geosynchronous satellite, respectively [Fig. 1-1].

The sizes for the solar panel and the body are assumed to be unknown. The observer is the sensor that measures the sunlight reflected by the solar panel and the body along the direction of the line of sight from the sensor to the satellite. The material constitutive laws of interest are the bidirectional reflectance distribution functions (BRDF) for diffuse and specular reflectances of the solar panel and the body. The reference frame is the Earth-Centered Inertial (ECI) reference frame [2]. The purpose of this analysis is to characterize the albedo-Area product of the panel and the body.

Any surface may be viewed as a collection of planar facets. An individual facet may be 2-D simplex (i.e. triangle) or a quadrilateral, which is a combination of two triangles. The size (area) of a triangle is half the magnitude of the cross-product of it sides. In geometry, the vector area can be defined for a finite planar surface using the scalar area and a unit vector that is normal to the plane of the surface. Albedo is a dimensionless quantity that equals the ratio of the reflected sunlight to incident sunlight. The albedo is defined in terms of a BRDFthat defines optical reflectance with respect to two vector directions; namely the vector direction of incident sunlight and the vector direction of the line of sight of the sensor. Thus, we may interpret the albedo-Area product as a vector. Or, in other words, the albedo-Area product of a satellite is a function of its pose with respect to the observer and not a scalar, constant value. We can also consider the albedo-Area product of a satellite as the sum of the albedo-Area products for the solar panels and the body.

The solar panel of a 3-axis stabilized satellite tracks the sun's projection in the equatorial plane. The axis of the solar panel is normal to the orbital plane of the satellite. The normal to the solar panel typically has an offset angle with respect to the direction of incident sunlight, which is assumed herein to remain constant over the duration of interval in which the observation data is analyzed. However, in reality, the solar panel offset angle may be changed by its operators from time-to-time. The body points to nadir in order to communicate with the terrestrial stations or customers. Thus, a 3-axis stabilized satellite can be visualized as an articulating assembly of the solar panels and the body. The relative orientation of the body with respect to the solar panels depends on the orbital position of the satellite. Thus, the satellite may be considered as an object with a periodic geometry.

The vector directions of incident and reflected sunlight can be defined in terms of the azimuth and elevation angles in a spherical coordinate frame attached to the center of mass of the satellite. These two vector directions are defined with respect to the normal of the particular surface under consideration, either the panel or the body. Consider the body's reference frame, Fig. 1-2. Let the first axis of the spherical coordinate frame be perpendicular to the orbital plane of the satellite and the second axis point to nadir. The third axis is defined to complete the orthogonal triad. Since the orbital position of the satellite and its geometry change continuously, the definition of the spherical coordinate frame with respect to the ECI reference frame changes continuously as well. As this coordinate frame is tied to nadir, the frame accommodates the angles relative to the body component, labeled as ψ and η. A similar coordinate frame tied to the solar panel normal may be established to accommodate the angles relative to the panel component, labeled ω and θ, shown in Fig. 1-3.[1]

Consider two instants of time. In general, for the two instants, the azimuth and elevation angles for the vector directions of incident and reflected sunlight with respect to the normal vectors to its solar panels and the body will be different. This change in the angles is due to two reasons, namely due to change in the relative position of the satellite with respect to the sensor and the sun and also due to the geometry and ephemerides of the satellite. Then, as per the PMFI, the optical reflectance behavior of the solar panel and body can only be a function of the vector

[1] The angles of observation, $\psi, \eta, \omega, and\ \theta$, are defined more precisely in Section 2.

directions of the incident and reflected sunlight with respect to the normal vectors to the solar panel and the body. It is insufficient to define the optical reflectance only as a function of azimuth angle or the elevation angle. Furthermore, finite angles are not vectors and thus we cannot define components of optical reflectance in terms of the azimuth angle or elevation angle.

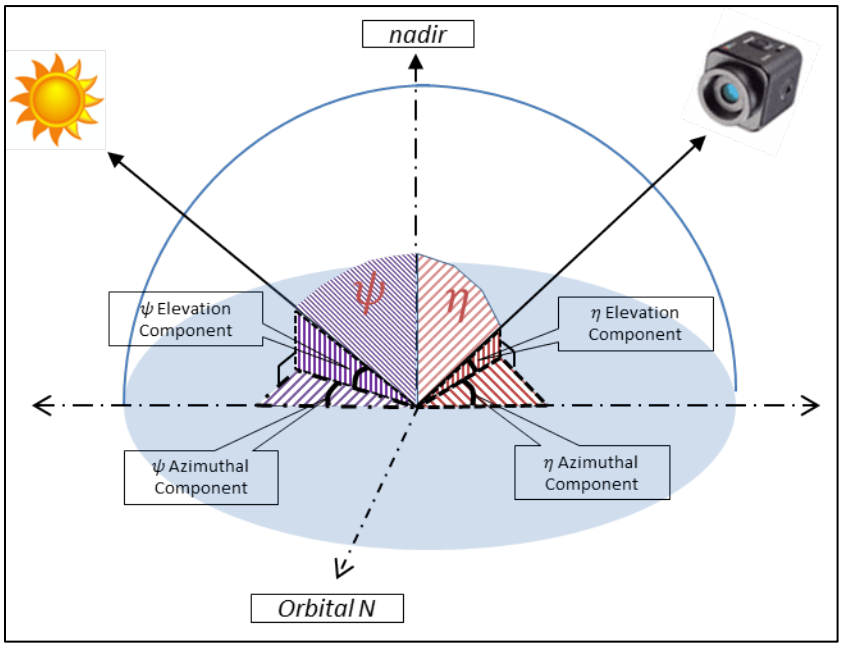

Fig. 1-2: Rotating Coordinate Frame Specific to the Body

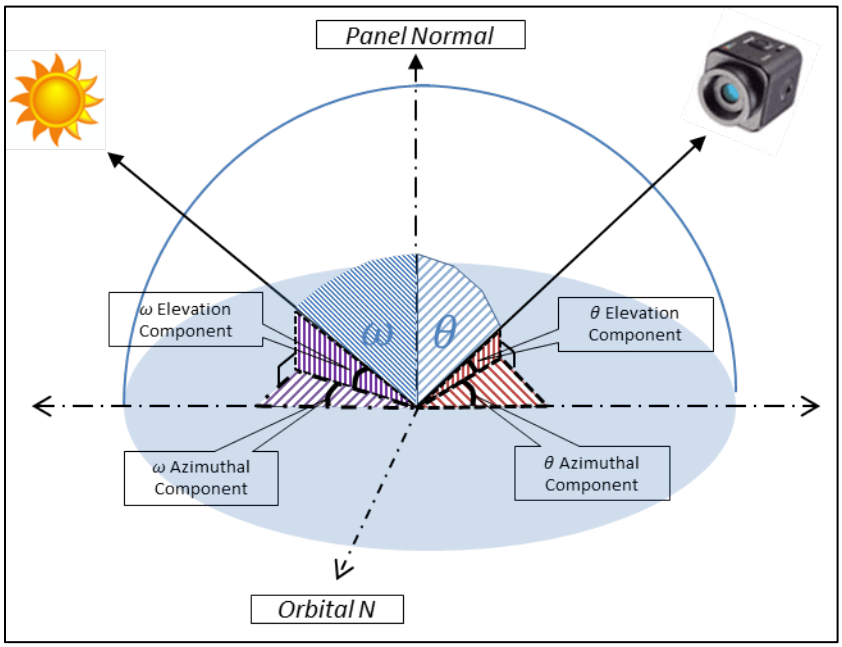

Fig. 1-3: Rotating Coordinate Frame Specific to the Panel

Once again, consider two instants of time that are distinct from each other. If the vector directions of the incident and reflected sunlight with respect to the normal to solar panel are identical at these two instants, then the contribution of the solar panel to the brightness of the GEO satellite at these two instants is identical. Or alternately,

the fraction of the albedo-Area for the satellite due to the solar panel will be identical at these two instants. This condition is denoted as an occurrence of a point pair for the solar panel. Similarly, if the two vector directions are identical at another two instants of time with respect to the normal vector to the body, then the contribution of the body to the brightness (or the albedo-Area) of the GEO satellite at these second two instants of time will be identical. This condition is denoted as an occurrence of a point pair for the body.

Consider that the albedo-Area of a satellite is a sum of the albedo-Areas of the solar panel and the body. Since the albedo-Area of the solar panel and body depend on the changing vector directions of the incident and reflected sunlight, the projected albedo-Area of the satellite changes continuously. The measured brightness of the satellite can be converted into its albedo-Area product. A convenient mathematical procedure for this conversion is described in[3]. Thus, each observation renders an equation that consists of one known (i.e. the projected albedo-Area of the satellite) and two unknowns (i.e., the intrinsic albedo-Areas of the solar panel and the body).

Consider a situation when we have observation data at two instants of time. If the two instants are close to each other, the two equations rendered by the two observations embody significant linear dependence and we cannot reliably solve for the two unknowns. If the two instants are distinct from each other, the two equations are linearly independent, but the projected albedo-Areas of the solar panel and the body change as well. Thus we are left with two equations and four unknowns, which is not useful. This difficulty is not resolved by collecting data in multiple wavebands because the number of independent equations grows in proportion to the number of wavebands, and the number of unknowns grows in proportion to twice the number of wavebands. The use of point pairing is meant to equalize the number of unknowns to the number of independent equations irrespective of the number of wavebands in which the data is collected.

Consider the situation when we have data at a point pair for the body. The location of a point pair can be found by mining an archive of brightness observations for a satellite. For example, such data is routinely collected in the open filter (panchromatic data) by the metric-photometric sensors as a part of their astrometry mission. Or a desired point pair of panchromatic or multi-color data may be collected by a priori determination of sensor tasking. With a point pair, we have two independent equations and three unknowns. It is necessary to eliminate one additional unknown. To this end, consider that the solar declination changes continuously. Its range is -23.5^{o} to $+23.5^{o}$. Due to the Earth's elliptical orbit, the variation of the solar declination changes faster in January than July. Since the perihelion and aphelion do not occur at the solstices, the maxima and minima are slightly asymmetrical [4] This results in the maximum change of declination at the equinoxes of roughly 0.4 deg/day and at the solstices there is virtually no change. Thus, we have a satellite with a periodic geometry and a gradual change in the vector direction of illumination. The definition of a body point pair is narrowed to include an additional condition that the equalization of body contribution be accompanied by a marginal change ($\sim 5^{o}$) in the vector direction of reflected sunlight for the solar panel. This marginal change need only be as large as that required to render the two equations linearly independent.

With the narrowed definition of a body point pair, we still have two independent equations and three unknowns. However, since the change in the vector directions for the solar panel is marginal, the two unknowns corresponding to the albedo-Area of the solar panel can be related to each other using the BRDF definition. This creates a set of three independent equations and three unknowns, which can be readily solved. The definition and solution procedure using a solar panel point pair is the counterpart of the logic described above for a body point pair [5].

The organization for the remainder of this paper is as follows. Section 2 describes the geometry of observation for a GEO satellite. Section 3 describes a two-facet model that represents the satellite in terms of a sun-tracking facet and a nadir-facing facet. Section 4 describes the reflectance and albedo-Area expressions based on the two-facet model. Section 5 describes the procedure for the solution of albedo-Area values for the solar panel and the body. Section 5

also shows a notional example for the identification of point-pairing conditions using the satellite two-line element (TLE) data. Section 6 lists the conclusions.

2. GEOMETRY OF TERRESTRIAL BASED OBSERVATION OF A GEOSTATIONARY RSO

Before proceeding further, a picture of the geometry of observation is useful. Consider the following diagram, Fig. 2-1. Note that the depiction is not to scale and is in 3D. The reference frame is ECI coordinates, where the origin is the earth's center, the vertical axis corresponds to celestial north, the horizontal axis passes through the equinoxes, and the third axis completes the orthogonal triad [2]. The observation station, shown as a purple point labeled "Obs," is at approximately $30°N$ latitude and at approximately 45° longitude off of the RSO's nadir vector, shown as a dotted black line. The RSO, shown as a blue point, is in a geostationary orbit, shown as a black circle, and its sunward articulating panel component is shown as a blue segment.

As the RSO orbits the earth, the panel component maintains alignment with respect to the sun's projection in the equatorial plane. The panel's normal ($\overrightarrow{P_\perp}$), shown as a green dashed vector, is offset by angle α from the projection of the sun. The light incident to the object arrives along the RSO-Sun vector ($\overrightarrow{RS}$), shown as an orange line. The angle between $\overrightarrow{RS}$ and $\overrightarrow{P_\perp}$, labeled ω, determines the panel's illumination per unit area, and the angle between the RSO-Observer vector ($\overrightarrow{RO}$) and $\overrightarrow{P_\perp}$, labeled θ, determines the panel's projected area from the observer's perspective. The angle, labeled β, between the panel specular reflection vector ($\overrightarrow{P_{spec}}$), shown as a light blue dot-dashed line, and $\overrightarrow{RO}$ determines the strength of the panel's specular glint from the observer's perspective.

While the panel component maintains constant alignment with the sun's projection into the equatorial plane, the RSO's body maintains a nadir facing orientation ($\vec{E}$). The angle between $\overrightarrow{RS}$ and $\vec{E}$, labeled ψ, determines the body's illumination per unit area, and the angle between $\overrightarrow{RO}$ and $\vec{E}$, labeled η, determines the body's projected area from the observer's perspective.

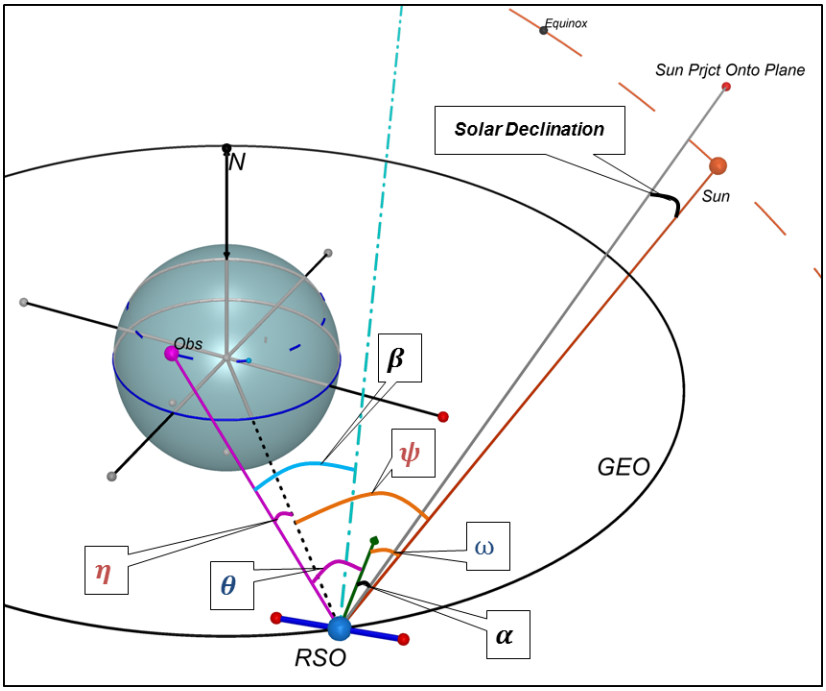

Fig. 2-1: Terrestrial Observation Geometry

3. TWO FACET MODEL OF A RESIDENT SPACE OBJECT (RSO) IN GEOSYNCHRONOUS ORBIT

Due to the complexity of a satellite's shape and motion, the system of equations that describe the satellite's properties is underdetermined, i.e. there are fewer equations than unknowns. However, most of these properties are negligible or can be aggregated to form a more accessible and universal model. It has been found that, in the case of three-axis stabilized satellites in a geosynchronous orbit, a two facet model performs adequately. In this section, the assumptions underlying this model are outlined.

3.1 ASSUMPTIONS

1. The space object has a *three-axis stabilized, nadir-pointing body*.
2. The space object has *sunward facing, articulating solar panels* that maintain a constant alignment with the projection of the sun in the equatorial plane, barring an operator maneuver or other non-nominal behavior.
3. The space object is represented by a *two-facet model*, in which one facet represents the solar panels and the other represents the body.
4. The panel facet is approximately planar and possesses both *specular* and *Lambertian* reflectance properties. Because it tends to zero away from the vector of specular reflection (glint), the specular component is only dominant within a glint region. Otherwise, the panel's contribution is dominated by Lambertian reflectance.
5. The body is a complex three-dimensional shape with approximately Lambertian aggregate reflectance. It has a different observed pose (due to self-occlusion) at each phase angle.

4. INTENSITY OF REFLECTANCE AND ALBEDO-AREA

Consider the solar energy in a certain waveband incident on the RSO and the intensity of its reflectance off of the RSO. If the RSO is observed as an unresolved point source, then the *radiant power*[2] of its reflection, denoted Φ (note this is an uppercase phi), is the total reflected solar energy per unit time originating from that point source, measured in units of $[W]$ [6]. The observed *intensity*, denoted I, of this reflectance, then, is the energy flowing through a solid angle centered at the source per unit time, measured in units of $[W/sr]$.

The intensity of an RSO's reflectance depends on three parameters that are assumed, at least in the near term, to be constant. These parameters are the incident *solar flux* in a certain waveband, denoted f_{sun} $\left[\frac{W}{sr\ m^2}\right]$ and sometimes referred to as the "solar constant," the *area* of the RSO's reflecting facets measured in units of $[m^2]$, and the *albedo* of the facets, which is unit-less. The last two parameters listed, area and albedo, are qualities intrinsic to the RSO's material. While it is impossible to determine those parameters individually without specific insight into the RSO's construction, their product, *albedo-Area* (aA), can be determined from photometric and astrometric data [3].

While aA is a property that is intrinsic to an object, the observed aA of an object at any given moment is a projection of its geometry of observation with respect to the source of illumination and the observer. "*Projected" aA* of an object, then, refers to its observed value based on the current geometry of the observation. *"Intrinsic" aA* of an object, on the other hand, refers to its value independent of the geometry of observation. For clarity, the symbol $\widetilde{aA}_x$ is used to represent an object x's projected aA, while the symbol $\boldsymbol{aA_x}$ is used to represent its intrinsic aA.

4.1 COMPOSITION OF THE TOTAL PHOTOMETRIC SIGNATURE

The power of the RSO's total reflectance at the point source is an aggregate of the respective powers of the panel and body reflectances, as shown next in (4-1).

$$\Phi_{RSO} = \Phi_P + \Phi_B\ [\boldsymbol{W}] \tag{4-1}$$

[2] Although this quantity is based in emissive radiometry, it is adapted for the reflectance photometry.

The RSO's observed intensity, however, is a projection through a solid angle of observation, shown next in (4-2).

$$I_{RSO} = I_P + I_B \ [\boldsymbol{W/sr}] \tag{4-2}$$

By the assumptions in Section 3.1, the panel's reflectance has both a Lambertian and specular component, as it is a roughly planar surface. The body, on the other hand, is a complex three dimensional object and is assumed to possess roughly Lambertian reflectance (as an aggregate of many small specular reflections). Equation (4-2) is now re-written as (4-3) with this in mind, where subscripts L and S denote "Lambertian" and "specular" respectively.

$$I_{RSO} = I_{PL} + I_{PS} + I_{BL} \ [\boldsymbol{W/sr}] \tag{4-3}$$

A specular reflection (sometimes called a "glint") may be thought of as a near perfect mirror-like reflection of the incident light, where the angle of reflection is equal to the angle of incidence. The strength of this reflection from the observer's point of view depends on the angle between the observer and the vector of specular reflection, defined earlier as β, where $\frac{\pi}{2} > \beta > 0$. Let I_{PS}, then, be written as a function of β, denoted $I_{PS}(\beta)$. As $\beta \to 0$, the specular contribution $I_{PS}(\beta)$ quickly becomes large since the vector of specular reflectance is aligning with the observation vector. As $\beta \to \frac{\pi}{2}$, however, the vector of specular reflectance and the observation vector are diverging, so, from the observer's perspective, the specular contribution $I_{PS}(\beta)$ decreases sharply. Equation (4-3) is now re-written in (4-4) as such a function of β.

$$I_{RSO}(\beta) = I_{PL} + I_{PS}(\beta) + I_{BL} \ \ [\boldsymbol{W/sr}] \tag{4-4}$$

The strength of the Lambertian reflectance of the panel is proportional to its projected brightness, contributing a factor of $\cos(\omega)$. It is also proportional to the projected area from the observer's perspective, contributing a factor of $\cos(\theta)$. Similarly, the strength of the Lambertian reflectance of the body is proportional to its projected brightness, contributing a factor of $\cos(\psi)$, and to its projected area from the observer's perspective, contributing a factor of $\cos(\eta)$. Equation (4-4) is now updated in (4-5).

$$I_{RSO}(\beta, \omega, \theta, \psi, \eta) = I_{PL}\cos(\omega)\cos(\theta) + I_{PS}(\beta) + I_{BL}\cos(\psi)\cos(\eta) \ [\boldsymbol{W/sr}] \tag{4-5}$$

Rather than consider the intensity of the RSO's reflectance, however, a transformation to projected albedo-Area ($\widetilde{aA_{RSO}}$) is performed from the photometric and astrometric data (apparent magnitude and position vectors). Because this method is defined for Lambertian only reflectance, only observations where β is not close to 0° are considered so that the specular contribution of the panel $I_{PS}(\beta)$ drops to near zero. This transformation, derived in previous work, is performed on (4-5) to obtain (4-6) [3].

$$\widetilde{aA_{RSO}} \approx aA_P\cos(\omega)\cos(\theta) + aA_B\cos(\psi)\cos(\eta) \ \ [\boldsymbol{m^2}] \ \ | \ while \ \beta \ is \ not \ close \ to \ 0° \tag{4-6}$$

Decomposing the total projected albedo-Area of an RSO (aA_{RSO}) into component intrinsic albedo-Areas ($aA_P \ and \ aA_B$) is a task fundamental to the characterization of the RSO. In the next section, a method of performing such a decomposition from both space based observations and a single ground based sensor is proposed.

5. POINT PAIRING

The fundamental goal of *Point-Pairing* is to obtain a pair of observation data points that possess a certain geometric compatibility allowing for the cancellation of either the body or panel component, leaving only the other component. The two observations should meet the following basic criteria.

In the case of *Body Point-Pairing*, in which the body's contribution cancels out, leaving only the panel's contribution, the following conditions must be met.

1. The body's contribution to the total projected albedo-Area should be identical for each observation.
2. The panel's contribution to the total projected albedo-Area should be different for each observation.
3. The observations must be made at identical longitudinal phase angles so that the body's poses are identical.

In the case of *Panel Point-Pairing*, in which the panel's contribution cancels out, leaving only the body's contribution, the following conditions must be met.

1. The panel's contribution to the total projected albedo-Area should be identical for each observation.
2. The body's contribution to the total projected albedo-Area should be different for each observation, while the body's observed pose should be identical.
3. The observations must be made at identical longitudinal phase angles so that the body's poses are identical.

An example of *body point-pairing* will be given from a simulated data set using a single ground based observer, while an example of *panel point-pairing* will be given from a simulated data set with a space based observer.

5.1 BODY POINT-PAIRING METHODOLOGY

Body Point-Pairing relies on the proposition that, for nearly every observation, another observation exists for which the projected body component is equal (within a certain tolerance), while the projected panel component is different. Furthermore, the body's poses in each of these observations must be identical. If two such observations are known, then the difference between the two observations is an expression containing only a projection of the panel component. Consider two such observations of the same RSO, defined mathematically next in (5-1).

$$\begin{gathered} aA_{RSO_1} = aA_P \cos(\omega_1)\cos(\theta_1) + aA_B \cos(\psi_1)\cos(\eta_1) \ \ [\boldsymbol{m^2}] \\ aA_{RSO_2} = aA_P \cos(\omega_2)\cos(\theta_2) + aA_B \cos(\psi_2)\cos(\eta_2) \ \ [\boldsymbol{m^2}] \\ such\ that \\ \psi_1 \approx \psi_2 \ and \ \eta_1 \approx \eta_2 \\ \omega_1 \neq \omega_2 \ or \ \theta_1 \neq \theta_2 \end{gathered} \tag{5-1}$$

The observations are subtracted, shown next in (5-2).

$$\begin{gathered} aA_{RSO_1} - aA_{RSO_2} \\ = \\ aA_P[\cos(\omega_1)\cos(\theta_1) - \cos(\omega_2)\cos(\theta_2)] + aA_B[\cos(\psi_1)\cos(\eta_1) - \cos(\psi_2)\cos(\eta_2)] \ \ [\boldsymbol{m^2}] \end{gathered} \tag{5-2}$$

Since $\cos(\psi_1)\cos(\eta_1) \approx \cos(\psi_2)\cos(\eta_2)$ by equation (5-1), the difference between the trigonometric products for the body is very close to zero. This allows the body component to drop out nearly completely when the difference is computed. Equation (5-2) may now be re-written in terms of just the panel's component, allowing the panel's intrinsic albedo-Area to be computed directly in equation (5-3).

$$\begin{gathered} aA_{RSO_1} - aA_{RSO_2} \approx aA_P[\cos(\omega_1)\cos(\theta_1) - \cos(\omega_2)\cos(\theta_2)] \ \ [\boldsymbol{m^2}] \\ \Downarrow \\ aA_P \approx \frac{aA_{RSO_1} - aA_{RSO_2}}{\cos(\omega_1)\cos(\theta_1) - \cos(\omega_2)\cos(\theta_2)} \ \ [\boldsymbol{m^2}] \end{gathered} \tag{5-3}$$

Since the body angles of observation, ψ and η, are very close from one observation to the next, the algebraic condition for the body's contribution to cancel out is met within a certain tolerance. Since satellite buses can vary greatly along the east-west direction, however, it is further required that the phase angle of the observations be nearly identical. This requirement ensures that the body is captured in an identical pose for each observation.

5.1.1 IMPORTANT CONSIDERATIONS FOR BODY POINT PAIRING

Although (5-3) provides a simple expression for the panel's intrinsic albedo-Area, caution must be taken in this approach. Consider the three main requirements established so far that are necessary for body point-pairing to be successful.

1. The body's contribution to the total projected albedo-Area should be identical for each observation.
2. The panel's contribution to the total projected albedo-Area should be different for each observation.
3. The observations must be made at identical phase angles so that the body's poses are equivalent.

Recall that the solar panel is assumed to articulate towards the sun's projection in the equatorial plane during the course of the RSO's orbit. Because the panel's motion is assumed to possess only an east-west degree of freedom, the panel is specifically assumed to track the projection of the sun in the orbital plane. If this is the case, it can be shown that the solar panel will, in fact, always have the same orientation with respect to the body at identical phase angles, provided that there is no other change in the system dynamic. This presents a problem because a *different* projection of the panel component is required between two observations of the same phase angle if the body point-pairing method is to work. An investigation into behavior of the angles of observation, however, provides clarity.

5.1.2 RELATIONSHIP BETWEEN ANGLES OF OBSERVATION FOR THE GROUND BASED CASE

Recall Fig. 2-1, which illustrates all angles relevant to ground based observations of a geostationary satellite. In this situation, the satellite is nearly fixed with respect to the observer, with any variation owing to an inclination of the RSO from the equatorial plane or to the declination of the sun. On the other hand, if the observer is space based, the position of the RSO is constantly changing in relation to the observer.

To illustrate the relationship between the angles of observations, two data sets were simulated from the published Two Line Elements (TLE) of a geosynchronous satellite. One data set was constructed for the space based situation, and another was constructed for the ground based situation. For the space based case, the observer is a satellite in a sun-synchronous low earth orbit, while, in the ground based case, the observer is based in Albuquerque, New Mexico. Data points were calculated at 5 minute intervals over 120 days (admittedly a much finer temporal spacing than would occur in reality).

Consider the following plots of the angles $\omega, \theta, \psi, and\ \eta$ vs. phase angle. This phase angle is actually the longitudinal phase angle, which is the projection of the total phase angle onto the equatorial plane. We have defined it such that it ranges from $-180°$ to $180°$ where $0°$ occurs when the projections of the observer, the sun, and the RSO onto the equatorial plane are collinear. Longitudinal phase angle serves as the independent variable against which the RSO's angles of observation $(\omega, \theta, \psi, \eta)$ are analyzed. Fig. 5-1 is a plot of the first night of ground based observations. The angles relevant to the panel component are plotted in blue, while the angles relevant to the body component are plotted in red. Note that the fine temporal spacing of the simulation resulted in the illusion of continuity.

In Fig. 5-1, the ground based case, ω, the angle between the RSO-Sun vector and the panel normal, appears to be nearly constant with respect to phase angle. As ω is based on the orientation of the solar panel with respect to the sun, this is to be expected since the panel's position relative to the sun's projection in the equatorial plane remains fixed. Additionally, η, the angle between the RSO-observer vector and the body normal (nadir), appears to be nearly constant. This too is expected in the case of a fixed ground based observer. The angles ψ and θ, on the other hand, vary with relation to the relative position of the sun and are thus both closely tied to phase angle. Recall that ψ is the angle between RSO-sun vector and the body normal (nadir), and θ is the angle between the RSO-observer vector and the solar-pointing panel normal.

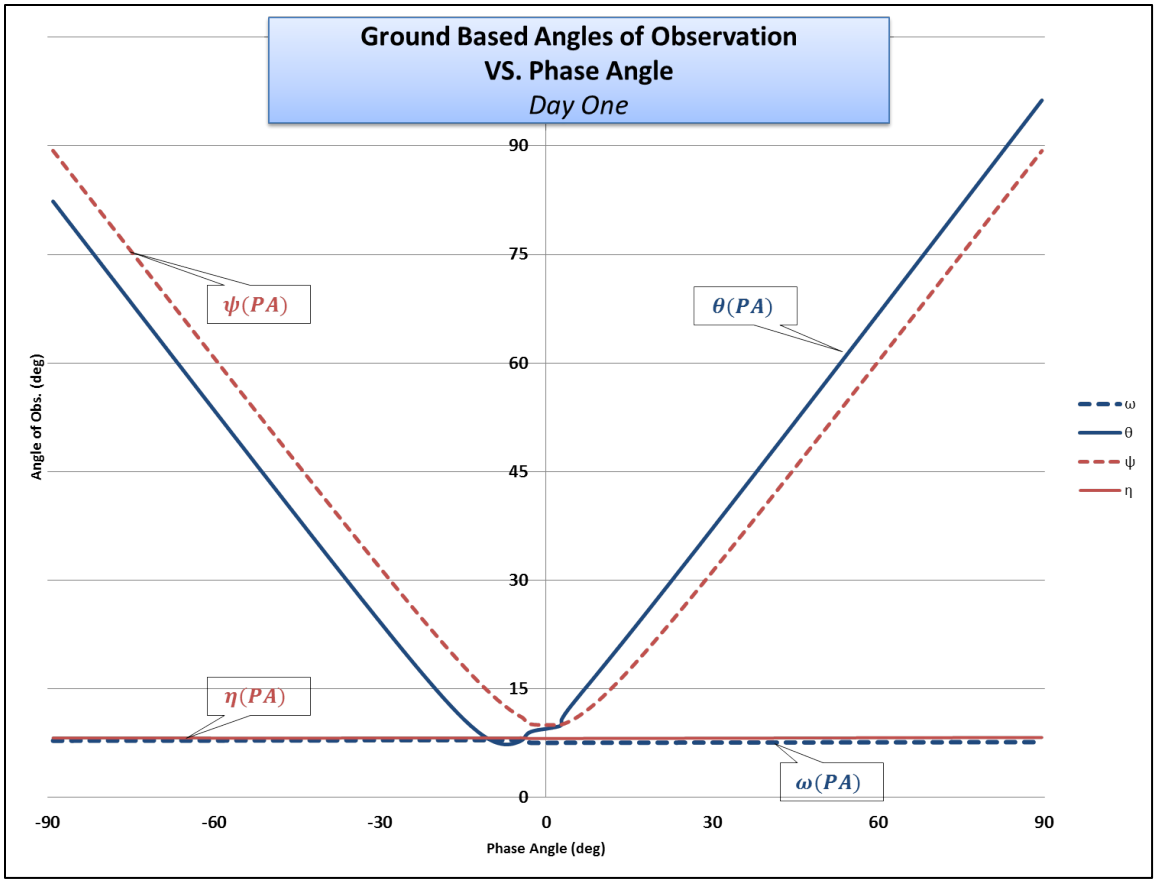

Fig. 5-1: Ground Based Angles of Observation VS. Phase Angle

Consider now plots of the same angles taken 15 days later. In Fig. 5-2, the second set of observations is overlaid against the initial observations so that the evolution may be observed. The curves from day one are subscripted as A, while the curves from day fifteen are subscripted as B.

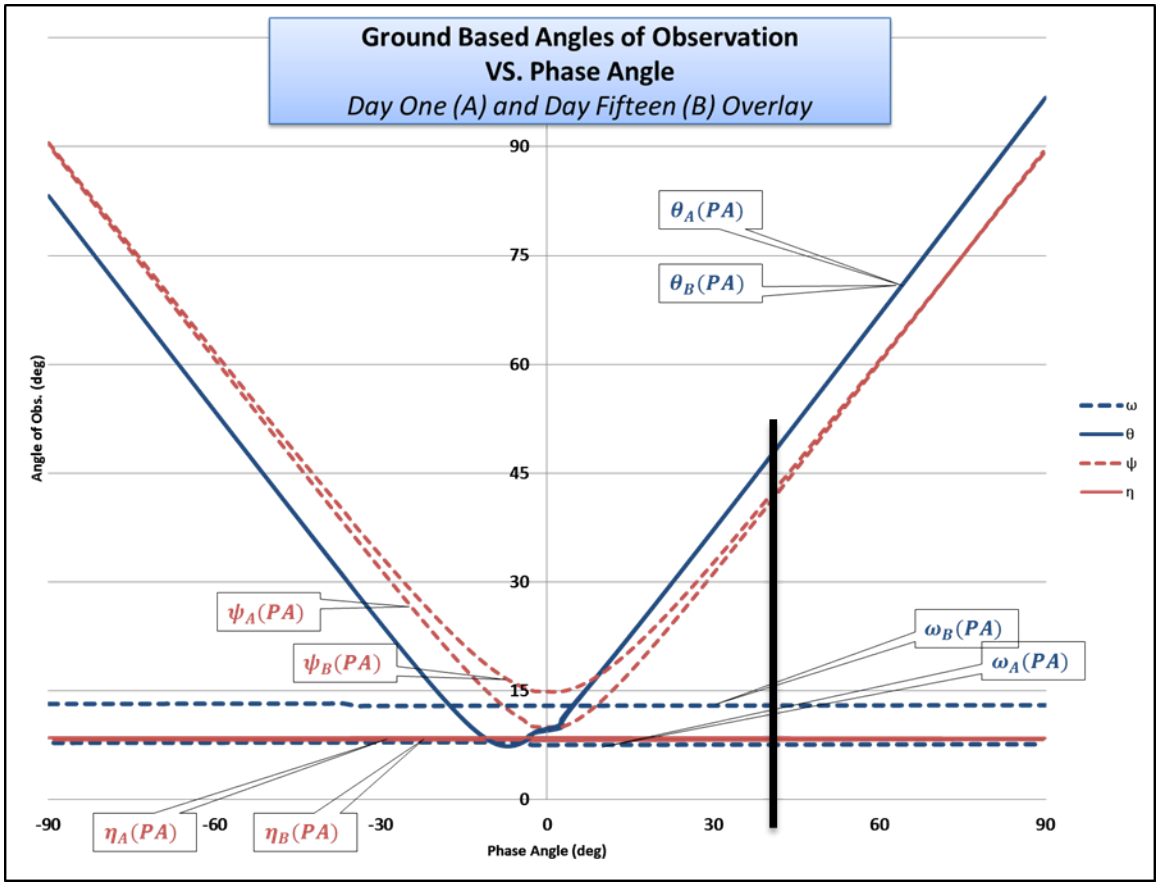

Fig. 5-2: Ground Based Angles of Observation 15 Day Overlay

In Fig. 5-2, the angle θ has nearly the same phase angle plot in both observations. In fact, since θ's azimuthal component is dependent on phase angle while its elevation component is dependent on solar declination, its phase angle plot will *only* change with solar declination. Furthermore, since the solar declination's range is much smaller than the phase angle's range and since it changes much more slowly, its overall effect on θ is relatively small.[3] Think of θ as the contributor to the east-west component of the panel's projected albedo-Area. A limitation of ground based point-pairing is now clearly illustrated: the difference required in the panel's projection *cannot be provided by* θ. On the other hand, consider the vertical translation of ω. Since ω is the angle between the RSO-Sun vector and the panel normal, it will remain fixed in the short term (in fact, its azimuthal component remains exactly constant barring operator intervention). However, since the sun changes declination throughout the year and the panel tracks the *projection* of the sun in the equatorial plane rather than the actual sun, ω will vary significantly throughout the year with declination. Think of ω as the north-south component of the panel's projection. It is ω, then, that provides the necessary diversity in the panel's projection for successful body point-pairing in the ground based case.

The black vertical line in Fig. 5-2 at approximately 40° phase angle illustrates a specific example of a *body point-pair*. From the plot, it can be seen that there exists a pair of observations at the same phase angle (ensuring an equivalent body pose) with nearly the same angles of observation for the body (ensuring algebraic equivalence of the body terms in the two-facet model within a certain tolerance), and a significantly different value for at least one

[3] Note that the inclination of the RSO to the equatorial plane also contributes to variation in θ, but this is usually small for geosynchronous satellites.

of the panel angles of observation, i.e. ω (ensuring linear independence). The albedo-Area of the panel component can now be computed by equation (5-3).[4]

5.2 PANEL POINT PAIRING METHODOLOGY

Panel point-pairing is similar to *body point-pairing* in that one component is cancelled out so that the other may be isolated. Specifically, two observations are found such that the panel's contribution to the total projected albedo-Area is the same. At the same time, the body's contribution to projected albedo-Area is different, while its pose is nearly the same from one observation to the next. Because the body's pose is required to be nearly identical, the phase angles of the observations must be close. The difference between the two observations will yield a measurement of the body's albedo-Area at the particular phase angle of the observations. Consider two such observations of the same RSO, defined mathematically next in (5-4).

$$\begin{gathered} aA_{RSO_1} = aA_P \cos(\omega_1)\cos(\theta_1) + aA_B \cos(\psi_1)\cos(\eta_1)\ \ [\boldsymbol{m^2}] \\ aA_{RSO_2} = aA_P \cos(\omega_2)\cos(\theta_2) + aA_B \cos(\psi_2)\cos(\eta_2)\ \ [\boldsymbol{m^2}] \\ such\ that \\ \omega_1 \approx \omega_2\ and\ \theta_1 \approx \theta_2 \\ \psi_1 \neq \psi_2\ or\ \eta_1 \neq \eta_2 \end{gathered} \tag{5-4}$$

The observations are subtracted (as in the *body point-pairing* case), shown next in (5-5).

$$\begin{gathered} aA_{RSO_1} - aA_{RSO_2} \\ = \\ aA_P[\cos(\omega_1)\cos(\theta_1) - \cos(\omega_2)\cos(\theta_2)] + aA_B[\cos(\psi_1)\cos(\eta_1) - \cos(\psi_2)\cos(\eta_2)]\ \ [\boldsymbol{m^2}] \end{gathered} \tag{5-5}$$

Since $\cos(\omega_1)\cos(\theta_1) \approx \cos(\omega_2)\cos(\theta_2)$ by equation (5-4), the difference between the trigonometric products for the panel is very close to zero. This allows the panel's component to drop out nearly completely when the difference is computed. Equation (5-3) may now be re-written in terms of just the body's component, allowing the body's intrinsic albedo-Area for the particular phase angle to be computed directly in equation (5-6).

$$\begin{gathered} aA_{RSO_1} - aA_{RSO_2} \approx aA_B[\cos(\psi_1)\cos(\eta_1) - \cos(\psi_2)\cos(\eta_2)]\ \ [\boldsymbol{m^2}] \\ \Downarrow \\ aA_B \approx \frac{aA_{RSO_1} - aA_{RSO_2}}{\cos(\psi_1)\cos(\eta_1) - \cos(\psi_2)\cos(\eta_2)}\ \ [\boldsymbol{m^2}] \end{gathered} \tag{5-6}$$

5.2.1 RELATIONSHIP BETWEEN ANGLES OF OBSERVATION FOR THE SPACE BASED CASE

Recall Fig. 2-1, in which the angles of observation for a terrestrial observer are illustrated. The angles of observation for the space based case are the same, and so the figure illustrates them correctly as well. The only difference is that the relative position between the observer and the RSO is not fixed. The effect this variation has on the angles' phase angle plots is explained presently.

In Fig. 5-3, the space based case, ω also appears nearly constant with respect to phase angle, as in the ground based case. As ω is not defined with respect to the observer, this continues to be in line with expectations. Similarly, angle ψ is not defined with respect to the observer either, so it shows nearly identical behavior to its ground based counterpart. Angles θ and η, however, *are* defined with respect to the observer, so the period of the observer's orbit contributes to their variation.[5]

---

[4] It is assumed that the changes to the material due to long term exposure to space are minimal over such a short period of time. Although this example uses 15 days, it is possible to find body point-pairs even closer that still possess an adequate change in the panel's projected albedo-Area.

[5] An observation satellite in sun-synchronous low earth orbit completes a revolution roughly every 90 minutes, which is about 16 full orbits for each 24 hour geosynchronous orbit.

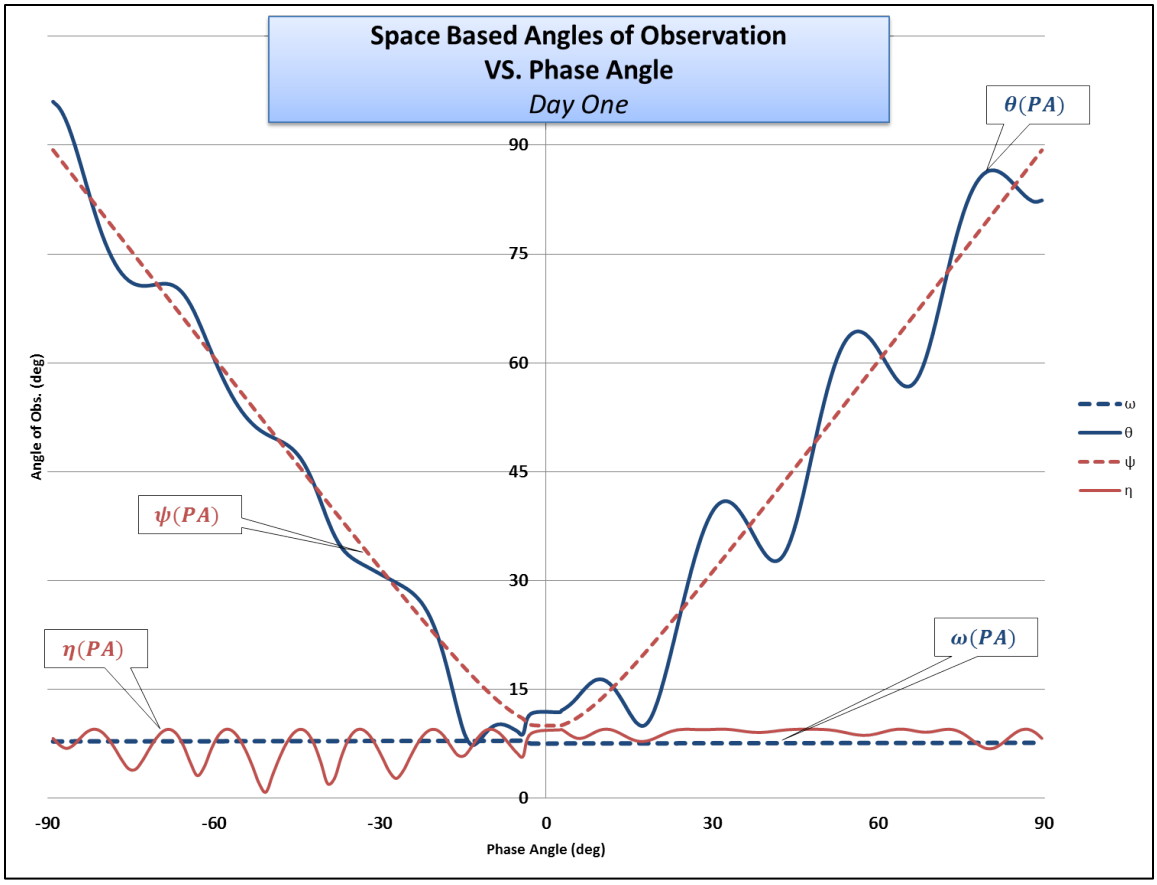

Fig. 5-3: Space Based Angles of Observation VS. Phase Angle

Consider Fig. 5-4, a scale magnification of the plot in Fig. 5-3 at 30° phase angle.

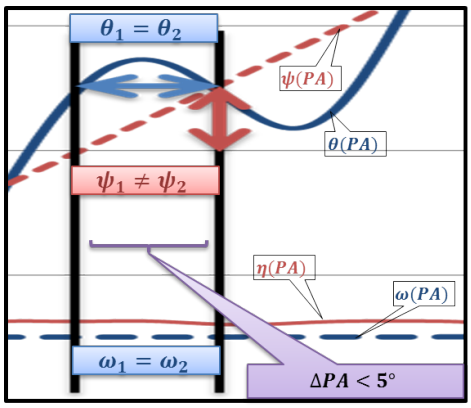

Fig. 5-4: Magnification of Space Based Angles of Observation Plot at 30° Phase Angle

Fig. 5-4 shows a pair of observations (indicated by the vertical black lines) which meet the *panel point-pairing* requirements. First, the two observations have a relatively close phase angle. The body's observed pose is therefore very similar. Secondly, the panel angles are equal for each observation: $\theta_1 = \theta_2$ *and* $\omega_1 = \omega_2$. At the same time, the body's projected albedo-Area is different between observations, since $\psi_1 \neq \psi_2$. The albedo-Area of the body at approximately 30° may now be computed by equation (5-6).

5.3 POINT PAIRING FINAL THOUGHTS

An example of *body point-pairing* was provided in the case of a single ground based observer that results in the projected albedo-Area of the panel. Although this method requires that there be several days between observations in the point-pair (note that the time between observations should be minimized), it adds a significant ability to gain insight into the decomposition of the RSO's total albedo-Area. Furthermore, note that geographic diversity provided by observation stations at different locations on the planet would enhance this methodology.

An example of *panel point-pairing* (resulting in the projected albedo-Area of the body) was provided in the case of a space based observer. In contrast to the case of the single ground based observer, a space based observer has the advantage of both longitudinal and latitudinal geographic diversity over a single diurnal cycle. This allows the point-pairing methodology to be performed on a much smaller time scale than in the case of the single ground based observer (a single diurnal cycle as opposed to 15 days). The ground based case, however, has the advantage of being more accessible and more easily tasked for specific observations that meet the point-pairing geometric requirements. Also, while it was not shown in this paper, *body point-pairing* is also possible for the case of a space based observer, and the observations can also be gathered in a single diurnal cycle.

6. CONCLUSIONS

This paper presents the procedure for the determination and use of point pair photometry data with respect to a ground-based sensor. Similar point pairing conditions can be determined for a space-based sensor. Although the point pairs are more prevalent in the space-based case due to the motion of the observer, sufficient conditions do exist in the case of a single ground based sensor by virtue of the change in solar declination.

The determination of body point pair data with respect to a ground-based sensor requires that either the solar panel offset angle or the RSO's inclination off the equatorial plane is nonzero. Another pathological condition is reached where the point pair for the body also corresponds to a point pair for the solar panel. The need for a non-zero solar panel offset angle is absent for space-based data due to its built-in geographic diversity.

Point pairing is performed independent of the waveband of observation. Thus if the data is collected in n-wavebands, the separation of the solar panel and body albedo areas is feasible in all n-wavebands. Indeed, in a notional case where point pairing data is collected by a hyperspectral sensor, the procedure described in this paper will render the material reflectance spectra for the solar panel and the body.

7. REFERENCES

1. Malvern, L.E., "Introduction to the mechanics of continuous medium", Library of congress catalog card number: 69-13712, Prentice-Hall, 1969, page 7.
2. Wikipedia, "Earth-centered inertial", URL: http://en.wikipedia.org/wiki/Earth-centered_inertial
3. Payne, T. E, Lucas, K., Chaudhary, A., Mutschler, S., Dao, P., Murray-Krezan, J., "A Derivation of the Analytical Relationship between the Projected Albedo-Area Product of a Space Object and its Aggregate Photometric Measurements", AMOS 2013 Technical Conference, Maui, HI.
4. Wikipedia, "Position of the Sun", URL: http://en.wikipedia.org/wiki/Position_of_the_Sun
5. Chaudhary, A.B., Payne, T.E., Gregory, S., Dao, P., "Fingerprinting of non-resolved three-axis stabilized space objects using a two-facet analytical model", AMOS 2011 Technical Conference, Maui, HI.
6. Tatum, Jeremy, "Stellar Atmospheres," http://orca.phys.uvic.ca/~tatum/stellatm.html, University of Victoria, 2011.